DETAILED STUDY OF FLOW STRUCTURE IN CFVN AND ITS EFFECTS ON THE FLOW RATE

E. von Lavante, H. Kaya, F. Winzösch and S. Brinkhorst,
University of Duisburg-Essen, Germany

Abstract

The flow fields in a toroidal Venturi nozzle shaped according to the ISO 9300 Standard, have been investigated using numerical flow simulation. The present study aimed at clarifying some of the phenomena associated with the unchoking of the throat. To this end, the shock structure has been studied for different Reynolds numbers and exit pressure ratios. The flow simulations were carried out in two and three dimensions. The flow fields were always unsteady, displaying a complex shock-boundary layer interaction.

Introduction

One of the simplest methods of highly accurate measurement of mass flows as well as volumetric flow rates at normalized conditions is the employment of critical nozzles. The guidelines and standards in using these devices are well defined and covered by the ISO Standard 9300 [1]. Its validity range is limited to Reynolds numbers between 10^5 and 10^7. However, even within these limits at the lower part of the range several investigators [2] [3] [4] have discovered flow effects that were not consistent with the simple quasi-one-dimensional theory. These included variation of the discharge coefficient C_D as a function of the nozzle back pressure not explainable by the theory offered in ISO 9300 [1], occurance of instabilities and pressure waves traveling upstream all the way through the throat and thus unchoking the nozzle for a very brief period of time, and the so called premature unchoking. After calibration, the corresponding nozzles still offer the same very reliable means of gas metering, however, as long as they are employed within their specifications. The flow fields in nozzles with Reynolds numbers below the range given by the standard ($Re = 1.0\ 10^3$ - $4.4\ 10^4$) have been investigated by von Lavante, Ishibashi and Wendt [5] experimentally as well as numerically.

More recently, Nakao and Takamoto [6] and Nakao [7] presented extensive studies of the chocking phenomenon aimed at shedding more light on this problem. The flow in a model nozzle has been simulated in two dimensions and compared to the corresponding experimental work in [8]. Generally, the comparison between experimental data and numerical results given in [8] is poor. As this work is seemingly related to the subject of the present paper, it will be discussed in more detail below. Finally, Mickan, Kramer and Li [9] not only present a plethora of experimental results related to the choking phenomenon, but also offer a plausible theory attempting to explain it. Unfortunately, some of their conclusions are based on the ill faited numerical simulations in [8]. Instead of using the somewhat ambiguose expression "premature unchoking" they suggest the more descriptive expressions "low unchoking" and "high unchoking", which the present authors will also employ.

The aim of the present work was to investigate the flow behavior in sonic nozzles in general, and the choking phenomenon in particular. To this end, the present authors have carried out several numerical flow simulations of one critical flow Venturi nozzle (CFVN) geometry in two and three dimensions. The Reynolds number was at this time fixed at Re_D = 140,000; however, the exit pressure ratio was varied between 0.2 and 0.8. The present investigators used the program ACHIEVE developed by the first author as well as the commercial code CD-adapco Star CCM+ (CCM+).

Numerical Methods

As the flow in the CFVN is always unsteady (if in doubt about this point, the interested reader is invited to listen to the CFVN operating - the noise is a clear indication of the unsteadiness), compressible and viscous, a corresponding solver had to be selected for the present work. Additionally, the flow could be either laminar or turbulent, depending on the Reynolds number.

The geometry of the nozzle has been mostly assumed to be two-dimensional axisymmetric, and in few cases plainly two-dimensional. The last assumption is almost certainly unrealistic in 99% of all the cases considered. However, it will be shown below that the flow in the nozzle is in significant parts of the diffuser of three-dimesional character.

The unsteady compressible viscous flow in the nozzles was therefore simulated using the Navier-Stokes solver ACHIEVE, developed by the first author. The code is based on Roe's Flux Difference Splitting in finite volume form employing a special quadratic van Albada limiter in order to minimize the numerical dissipation. The details of this code can be obtained from, for example, von Lavante and Grönner [10]. Traditionally, this code was by far superior to any commercial program in being able to resolve the complex flow structure in the CFVN. However, the recent version of the commercial program CCM+ proved to be able to give results that were comparable to those of ACHIEVE, providing an easy to use option to ACHIEVE. The coupled solver (compressible flow solver) is equally based on the Roe's averaging, which explaines its quality of results, although the details of this code are not publicly available.

Computational grids of good quality were essential for obtaining any results; here, the local resolution, grid stretching and cell skweness were important. The present grids consisted of between 17600 cells (coarse) and 122160 cells (fine) arranged in 3 to 4 blocks in two dimensions and 2.245 M cells in 4 blocks in three dimensions.

All of the present computations were carried out for the same geometry and inflow conditions. Here, a Venturi-nozzle according to ISO 9300 was taken, with a diffuser half angle of 4^o , diffuser length of 7 D^* (diameter at the throat) and D^* = 9.89 mm. The working fluid was air given at the inflow at P_{00} = 0.101325 MPa and T_{00} = 300 K.

Equally important are proper boundary conditions. The solver ACHIEVE is provided with genuinely non-reflective inflow and outflow boundary conditions. In CCM+, the non-reflective boundary conditions work only with steady flow; therefore, the outflow region had to be designed as a "dump" of pressure waves with ever increasing grid spacing for effective damping. Details of the boundary condition formulation in ACHIEVE can be found in, for example, Yao [11].

Two-Dimensional Results

Normal Shock in Outflow

In [9], it was shown that the mass flow displays in many cases a lower value than critical at a relatively low outflow pressure ratio p_{out}/P_{00} (ratio of static pressure at the end of the diffuser to the inflow total pressure), defined in [9] as low unchoking. It appeared at approximately p_{out}/P_{00} = 0.3 - 0.6, which corresponds to a flow condition at which a normal shock forms just at the exit from the diffuser. In the present case, the theoretical outflow pressure ratio according to a simple quasi-one-dimensional theory was 0.31. For comparison, a pressure ratio p_{out}/P_{00} =0.2 for smooth outflow was also simulated.

The simulations were performed by both ACHIEVE and CCM+.

At p_{out}/P_{00} = 0.31, a normal shock formed indeed in the diffuser; it was, however, always unsteady, forming inside the diffuser and moving to the outflow location and, after bypassing it, further downstream within the free jet. Eventually, it dissipated to a pressure wave that was passed out of the computational domain. Upstream of the exit shock, a complex lambda-shock-boundary layer interaction with massive unsteady flow separation was present, with the lambda-shock moving upstream and the normal exit shock moving downstream.

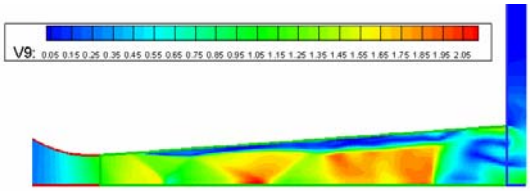

Fig. 1: Mach number contours, p_{out}/P_{00} = 0.31

In Fig. 1, the normal shock moving downstream as well as two lambda-shocks moving upstream can be viewed. Clearly visible is also the massive separation induced already by the first leg of the first shock. A detailed view of the first lambda shock at an earlier time (the shock being downstream of its location in Fig.1) can be seen in Fig. 2. Here, the stream lines are shown as well, making the determination of the deflection angle and the wave angle possible. The deflection was measured as $\delta=9^o$ and the wave angle $\beta=34^o$.

The Mach number ahead of the normal shock at the center line was M_x = 1.9, the one after the shock M_y = 0.50. The later value was somewhat low, but it should be recollected that the shock is moving in upstream direction.

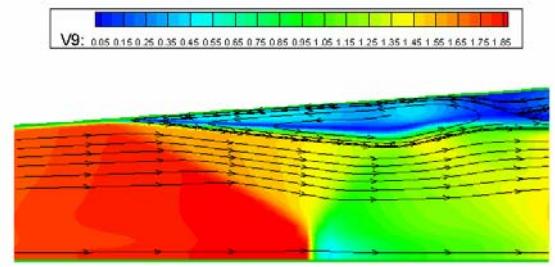

Fig. 2: Detail of the first lambda shock

The above values can be compared to the theoretical results given by the quasi-one-dimensional theory, to be found in, for example, NACA report 1135 [12] - **but not for the two-dimensional oblique shock !!!** The flow is definitely axisymmetric (how many of us have seen two-dimensional wedge-type CFVN??), so that the conical solution of the oblique shock relationships has to be taken. Unfortunately, [8] and [9] have based their discussion on just that, the wedge-type shock solutions. Fig. 3, taken from the NACA 1135 [12], shows the difference between the two solutions.

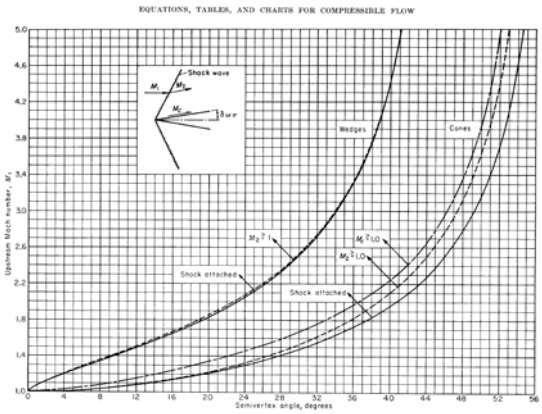

Fig. 3: Comparison of oblique shock results between two-dimensional shock and conical shock, from [12].

The present results given by the program ACHIEVE agree fairly well with the present three-dimensional results, given in a chapter below.

As the total pressure is a direct indication of the losses and closely coupled to the determination of the entropy, it should be considered presently. In Figure 4, the total pressure ratio P_t /P_{00} , where P_t was the local value of the total pressure and P_{00} was the total pressure at the inlet, is displayed for the flow field in Figure 1. As expected, the pressure ratio P_t/P_{00} remains below one.

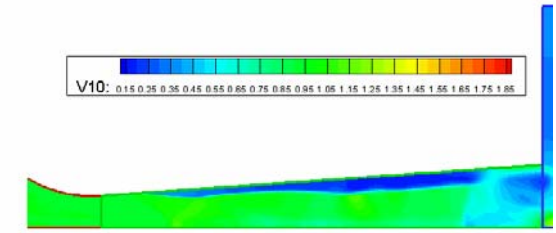

Fig. 4: Total pressure ratio P_t/P_{00} for the flow field in Fig. 1.

At a later time, the normal shock passes the exit and moves through the free jet downstream, forming a Mach-disk. In the diffuser, the first lambda shock moved all the way upstream, and downstream of the second lambda shock, a new normal shock is forming. Although moving in the positive flow direction, it is fairly strong as the Mach number ahead of it was in access of 2.35.

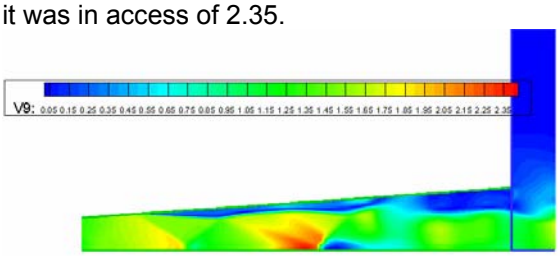

Fig. 5: Mach number contours, p_{out}/P_{00} = 0.31.

Again, the a large separated zone at the upper boundary is noticable. The corresponding plot of total pressure ratio bears some surprises.

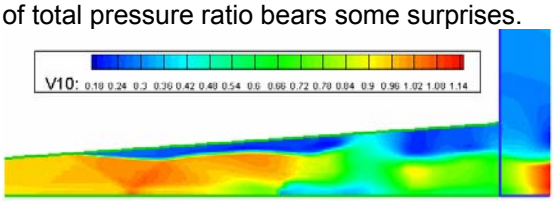

Fig. 6: Total pressure ratio P_t/P_{00} for the flow field in Fig. 5.

The total pressure increases across the shocks!! This seeming violation of the second law of thermodynamics was fist puzzling (the first author freely admits this moment of weakness), more so as most of the calssical lectures on gas dynamics do not mention this effect. The first indication that an increasing total pressure across moving shocks is possible was found in an unassuming but highly practical book by Zucker [13]. Consequently, the present authors undertook a little study of the total pressure ratio development as a function of the Mach number ahead of a moving shock M_1 and the Mach

number of the shock movement M_S . Taking first the total pressures relative to the moving shock (relative system), no unexpected results are obtained, Fig. 7. The ratio P_t / P_{00} remains below 1.0 and approaches 1.0 as the Mach number M_1 is approaching 1.0 as well.

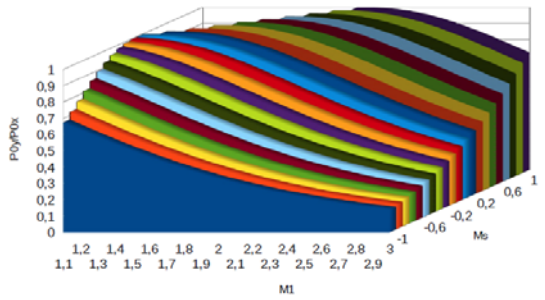

Fig. 7: Total pressure ratio P_{0x} / P_{0y} relative to the moving shock.

Taking, however, the total pressure ratio P_t / P_{00} in the absolute reference frame, relative to the stationary observer, a totally different picture is obtained, see Fig. 8.

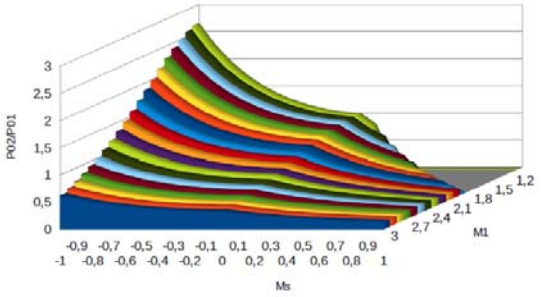

Fig. 8: Total pressure ratio P_t / P_{00} relative to a stationary observer.

The total pressure ratio in the case of negative shock Mach numbers (as present in Fig. 5) reaches well over 1.0. Clearly visible is also a ridge of values close to 1.0 extending diagonally across the diagramm, marking the situation where the relative Mach number ahead of the shock is nearly 1.0.

Mass Flow as a Function of Outflow Pressure Ratio

In the next study, aimed at supplementing and, if possible, providing further explanation to the theoretical frame work postulated in [9], the flow in the same nozzle as employed in the previous chapter was studied for different pressure ratios at the outflow from the diffuser, p_{out} / P_{00} . Again, the Reynolds number was Re_D=140,000, implying that the flow in the nozzle was predominantly laminar. As the low unchoking was expected at pressure ratios p_{out} / P_{00} between 0.3 and 0.6, the present work included following pressure ratios p_{out} / P_{00} : 0.20, 0.25, 0.30, 0.35, 0.40, 0.50, 0.60 and 0.70. In this study, only the commercial code CCM+ was used, as it proved to be capable of delivering results of similar quality as those obtained by ACHIVE. The resulting mass flow can be seen in Figure 9.

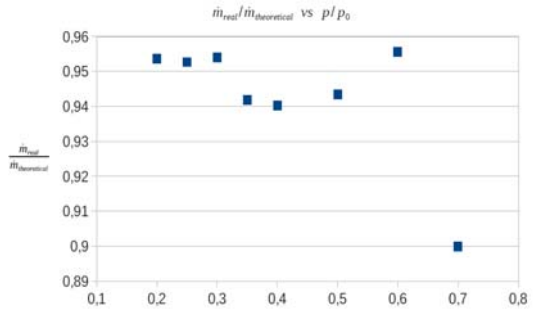

Fig. 9: Computed mass flow through the nozzle throat as a function of p_{out} / P_{00}.

The mass flow through the nozzle throat, as obtained from spatial and time-wise integration at the throat, displayed the same behavior as the experimental data described in [9]. For all the pressure ratios the flow was unsteady, with shocks moving within the diffuser and beyond. One should expect this results in the view of the massive separation caused by the shocks. Extensive separation like the one shown in Fig. 2, for example, will be neither steady nor symmetric.

The flow field in the case of p_{out} / P_{00} = 0.2 can be considered in Fig. 10.

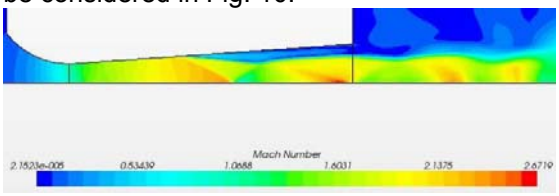

Fig. 10: Mach number contours, p_{out} / P_{00} = 0.2

The flow field displays no strong almost normal shocks, the oblique shocks were moving within the containment of the diffuser and never reached the throat. Consequently, the mass flow rate was approximately equal to the rate given by the Standard ISO 9300. The coresponding plot of the wall shear stress (blue, left scale) and entropy (red, right scale) at the wall is given in Figure 11. It is interesting to note that, as expected, the wall shear stress reaches its maximum in the throat, and its minimum in the separated region. The entropy increases all the way to the first leg of the lambda shock, then increases sharply in the

shock and falls off after the shock. The steep decrease is at first difficult to grasp; however, Figure 2 helps to explain this phenomenon. Entropy is an intensive property, transported by particles along streamlines. In the case of the separated flow in Figure 2, the streamlines originated all the way downstream in the low Mach number region above the free jet, in the "reservoir" of low entropy fluid, transporting it upstream through the separated boundary layer.

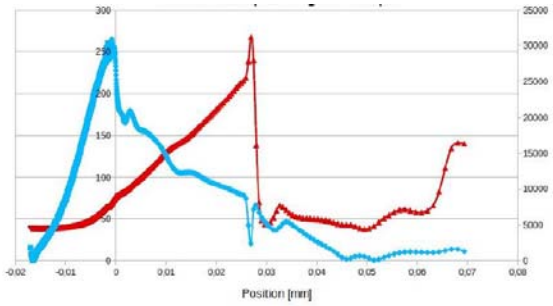

Fig. 11: Wall shear stress and entropy at the wall for flow given in Fig. 12.

The flow field in one instant of time for the ratio p_{out} /P_{00} = 0.35 is shown in Figure 12. As in the simulations performed by ACHIEVE, a system of two lambda shocks followed by an almost normal shock can be observed.

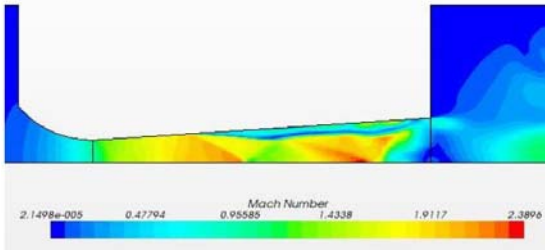

Fig. 12: Mach number contours, p_{out} /P_{00} = 0.35

The corresponding plot of the wall shear stress and entropy are displayed in Figure 13.

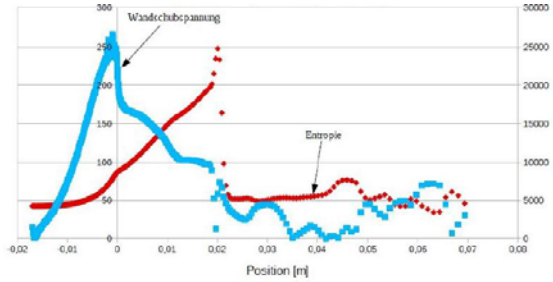

Fig. 13: Wall shear stress and entropy at the wall for flow given in Fig. 13.

As already stressed above, it was found that the flow fields were in all cases unsteady. However, as long as the unsteady movement of the shock systems was limited to the diffuser and did not reach the throat, the mass flow was approximately constant, corresponding to the choked condition. Even in this case, the pressure fluctuations could propage from the diffuser upstream through the boundary layer, resulting in small changes of the mass flow - an effect observed also experimentally. The low and high unchoking was the result of the shock system, changing from lambda-shock to a weak normal shock, in upstream direction through the throat. The shock movement is the result of complex interaction of the shock system with the boundary layer, being mainly effected by the always present separation. Additionally, it is expected that for cases with the Reynolds number Re_D close to 10^6 (the limiting value at which the transition from laminar to turbulent takes place in the throat or upstream of it) the shock-boundary layer interaction will also initiate transition, complicating matters even more. More on this subject can be found below in the chapter "Discussion of the results".

Three-Dimensional Results

In view of the massive unsteady boundary layer separation, the flow field will not most likely remain axisymmetric due to stochastic fluctuations within the separated region. Besides, several investigators have experimentally found asymmetric shock systems even in symmetric geometries. Therefore, it is expected that the real flow in the CFVNs will be most certainly of three-dimensional character. The present authors realized this fact and accounted for it by carrying out a three-dimensional flow simulation again within the same nozzle as used in the previous two studies.

At the time being, the commercial solver CCM+ was rendered suffucient for this numerical work. The grid, consisting of 2.245 M cells arranged in 4 blocks was generated using the commercial program GRIDGEN. No turbulent model was implemented as the Reynolds number was low at Re_D = 140,000, implying mostly laminar flow. The outflow pressure ratios imposed on the diffuser were , p_{out} /P_{00} = 0.7, 0.5 and 0.4.

As in all the two-dimensional simulations, the flow was unsteady for all three pressure ratios. The flow fields in the x-y plane along the geometric symmetry line are presented in Figure 14 for comparison as Mach number contours. Again, a shock structure consisting of at least two lamba-shocks and possibly a

terminating normal shock can be seen. As in the two-dimensional case, the first lambda shock induces boundary layer separation.

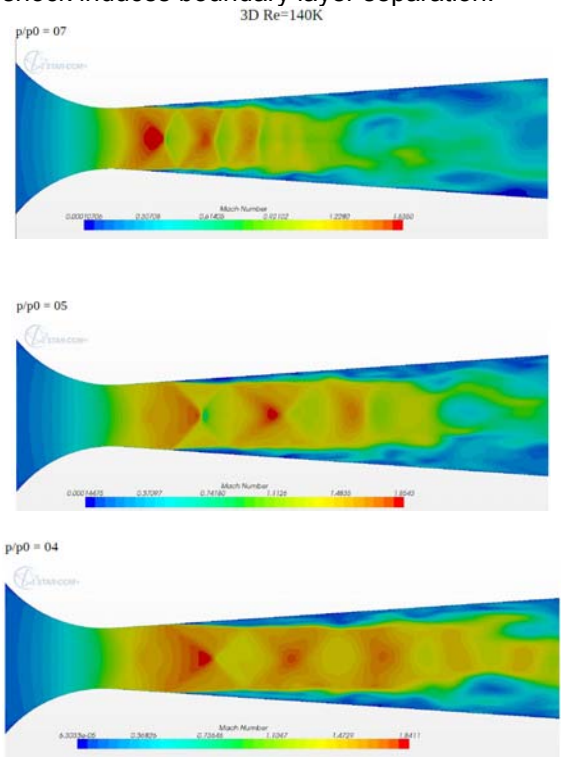

Fig. 14: Mach number contours for the three-dimensional results along a symmetry-plane for three different pressure ratios , p_{out} /P_{00}

As can be seen in Figure 14, the wave angle of the first lambda shock is decreasing with decreasing outflow pressure. The deflection angles were ϑ = 9°, 8° and 6° , respectively, agreeing well with the theory of conical shocks. The shock itself is moving downstream with decreasing outflow pressure. The separated boundary layer after the first shock is unsteady; the amplitude of the fluctuations is growing as the diffuser exit is approached. It was observed that the separated layer is not only moving in radial direction, but also rotating in tangential diection, creating a rather complex flow field as it is interacting with the shocks in the core flow.

A three-dimensional view of the flow is offered in Figure 15. The corresponding mass flow can be seen in Figure 16. It agrees well with the two-dimensional results, showing the tendencies described in the previous chapter. At approximately , p_{out} /P_{00} = 0.4, it displays a clear sign of low unchoking, again, due to unsteady movement of the lambda shock upstream all the way through the throat.

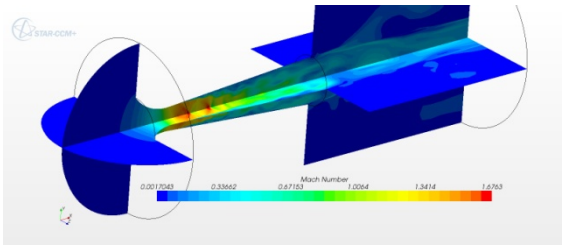

Fig. 15: Three-dimensional view of the Mach contours, p_{out} /P_{00} = 0.7

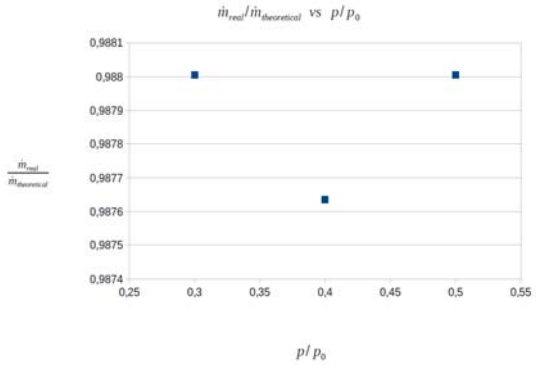

Fig. 16: Mass flow ratio (C_D -coefficient) of the three-dimensional computations.

Currently, the three-dimensional flow simulations are being carried out for a grid with approximately 4 Mcells.

Discussion of the Results

The present results must be considered in view of the more recent findings by other investigators. They were aimed at supporting the theoretical framework set by Mickan, Kramer and Li [9]. However, they seem to be accomplishing just the opposite, rendering some of the assumptions made in [9] as not realistic.

The discussion in [9] is based on the numerical and experimental results presented in [8]. There is the problem - the nozzle investigated in [8] was "two-dimensional", consisting of plane side walls and wedge-type upper and lower walls. Including the always present corner flow, this configuration is totally different from the axisymmetric CFVNs used in flow metering, being of hardly any significance. The numerical simulations in [8] are of poor quality; the two-dimensional assumption is not valid even on the symmetry line and the turbulence model (k-ω) way too dissipative for the present application. The authors admit that the numerical results were steady despite the experimental data indicating unsteady flow.

Much better basis for further theoretical considerations than [8] is the work by Deck, Hallard and Guillen [14], published 5 years prior to [8]. Here, both a two-dimensional and a three-dimensional axisymmetric nozzles have been studied. The numerical flow simulations included two-dimensional simulations, three-dimensional simulations in the two-dimensional geometry and three-dimensional simulations in the "real" axisymmetric nozzle. The shadow-graph of the lambda-shock in the two-dimensional nozzle ontained by [14] can be seen in Figure 17.

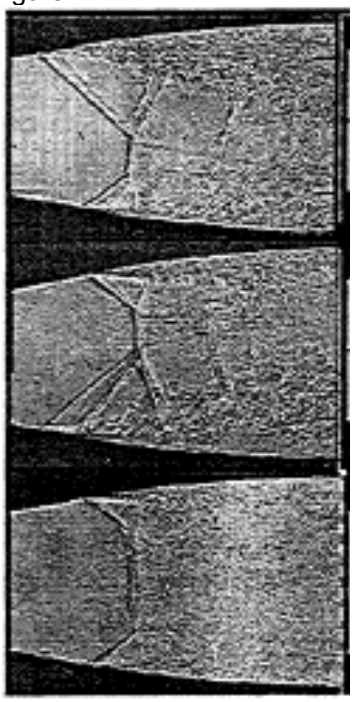

Fig. 17. Shadowgraph of the lambda shock in two-dimensional nozzle, from [14].

In all three pictures, the instability is induced by the first leg of the lambda shock, as expected. It is triggering large scale turbulence; however, its character could be described only after a proper analysis of the scales of the structures and the spectrum within the layer. The second leg of the lamba shock is further enhencing the unsteady movement within the layer between the separated region and the core flow. The instab ility is definitely not amplified or even initiated by the expansion waves that result from the reflection of the shock from the oposite wall. Expansion always stabilizes the flow, and this is obviously the case here; the expansion wave system decreases the thickness of the separated region. he pictures oin Figure 16vshow another feature of the lambda shock very nicely - the slip line from the Mach tripple point. The flow along this line has continuous pressure in direction normal to it, and the velocities on both sides are parallel, but the entropy, density and parallel velocity display a jump across it. Again, in presence of viscosity, the slip line is a location of a shear layer, destabilizing the flow.

Significantly, the authors in [14] emphasise that even on the symmetry line, the results of numerical flow simulation for the two-dimensional nozzle computet in 2-D and 3-D fashion are vastly different.

Conclusions

The present work offers one major conclusion: both the low and the high unchoking is the result of unsteady shock-boundary layer interaction, possibly coupled to laminar-turbulent transition. In terms of numerical prediction of the flow field, the present authors see a chance to obtain realistic results in all comprehensive three-dimensional large eddy or even direct simulation. The corresponding computational effort is extremely large due to the required spatial and time-wise resolution.

However, the usefulness of this effort seems somewhat questionable in light of some of the experimental results presented by Mickan, Kramer and Li in [9]. The resulting mass flow data for the same size, same operational conditions CFVNs of different manufacture displayed very different behavior, the only difference being the inside surface quality of the nozzles.

References

[1] International Standard ISO 9300, "Measurement of gas flow by means of critical flow Venturi nozzles", First Edition, Beuth, Berlin 1990.

[2] von Lavante, E., Nath, B. and Dietrich, H., "Effects of Instabilities on Flow Rates in Small Sonic Nozzles", Proceedings of the 9th Int. Conference on Flow Measurement FLOMEKO'98, Lund, 1998.

[3] Wendt, G., Ph.D. Thesis, University of Essen, Germany, 2000.

[4] Nakao, Shin-ichi, "Choking Phenomenon of Sonic Venturi Nozzles on Low Reynolds Numbers", Proceedings of the 9th Int. Conference on Flow Measurement FLOMEKO'98, Lund, 1998.

[5] von Lavante, E., Ishibashi, M., and Wendt, G., "Investigation of Flow Fields in Small Sonic Venturi.Nozzles", Proceedings of the 10th Int. Conference on Flow Measurement FLOMEKO'2000, Salvador, 2000.

[6] Nakao, S.-I. and Takamoto, M., "Chocking Phenomena of Sonic Nozzles at Low Reynolds Numbers", FMI 11, 2000.

[7] Nakao, S.-I., "High Pressure Hydrogen Gas Flow Measurements by the Critical Nozzle Flow Meter", 3rd Workshop on Critical Nozzles, Quedlingburg, Germany, 2005.

[8] Xiao,Q., Tsai, H. M. and Papamoschou, D., "Numerical Investigationof Supersonic Nozzle Flow Separation", AIAA Journal xxxx.

[9] Mickan, B., Kramer, R. and Li, Ch., "Critical Back Pressure Ratio in Sonic Nozzles - the Correlation with Diffuser Geometry and Gas Composition", 8th ISFFM Conference, Colorado, June 20-22, 2012.

[10] von Lavante, E. and Grönner, J., "Semiimplicit Schemes for Solving the Navier-Stokes Equations", 9th GAMM Conference, Lausanne, Notes on Numerical Fluid Mechanics, Vieweg, 1992.

[11] Yao, J., Ph.D. Thesis, University of Essen, Germany, 1999.

[12] NACA Report 1135, Ames Aeronautical Laboratory, 1953.

[13] R. D. Zucker, "Fundamentals of Gas Dynamics", Matrix Publishers Inc., 1977.

[14] Deck,Sebastien, Hallard,Remi, and Guillen, Philippe, "Numerical Simulations of Steady and Unsteady Separated Nozzle Flows", AIAA Paper 02-0406, 40th Aerospace Sciences Meeting, 2002.